AREAS DENOTE NO ERECTION OF DWELLINGS ALLOWED

"DEVELOPMENT APPLICATION" PURPOSES ONLY

UPPER HUNTER HOLDINGS PTY LIMITED

PROPOSED RURAL SUBDIVISION OF LAND AT "HOLLYDEEN" & "DOLWENDEE" SECTION 96 AMENDMENT TO ORIGINAL DA LOT LAYOUT

ACCESS POINT TO LOT 8

PROPOSED ACCESS TRACK TO 2WD STANDARD. RIGHT OF CARRIAGEWAY 10 METRES WIDE.

ACCESS FOR LOT 7

EXISTING ACCESS OFF HIGHWAY

EXISTING ACCESS OFF HIGHWAY TO SERVICE BOTH LOTS 4 &5

EXISTING ACCESS OFF HIGHWAY FOR EXISTING HOUSE

WYBONG

HOLLYDEEN

GOLDEN HIGHWAY

SANDY HOLLOW

DENMAN

REEDY CREEK ROAD

RIVER

Creek

Rocky Ground

Yards

Well

Pump

Tank

Dam

"Hollydeene"

"Dolwendee"

"Castlereagh"

BANK

IS BOUNDARY

EXISTING FENCE

EXISTING TRACK

VARIABLE WIDTH

8
40ha

7
76ha

6
86ha

5
44.37 ha

4
40.62 ha

3
40.58 ha

2
41.53 ha

Pt. 1

1
40.3ha

Revision No. : 1	Drawing File : S4953DA_PLAN_SEC96_2.dwg
Revision Information : ALTERNATIVE ROUTE FOR RIGHT OF CARRIAGEWAY	Survey Data File : S4953.Cc5
NOTE:- DIMENSIONS & AREAS ARE SUBJECT TO A FINAL SURVEY & REGISTRATION OF A DEPOSITED PLAN AT THE NSW LAND TITLES OFFICE	Date : 14th APRIL 2009
Liability Limited by a Scheme Approved under Professional Standards Legislation	Scale : AS SHOWN
COVER OF EXCELLENCE	Datum : MGA/AHD
	Drawn : RH Checked : PS

Boardman Peasley Pty Limited
Consulting Surveyors & Engineers
(Ph) 02 65 433600
(Fax) 02 65 425957
44 Market Street
Muswellbrook NSW 2333
P.O. Box 404
WWW.BOARDMANPEASLEY.NET.AU

UPPER HUNTER HOLDINGS PTY. LIMITED
PROPOSED RURAL SUBDIVISION OF LAND AT "HOLLYDEEN" & "DOLWENDEE"
SECTION 96 AMENDMENT TO ORIGINAL DA LOT LAYOUT

Sheet No. 1 of 1 Sheets
Job No. S4953
Plan No.

Attachment 9: Atmospheric Environment (NO_x Emission from Blasting Operations in Open Cut Coal Mining)

Atmospheric Environment 42 (2008) 7874–7883

Contents lists available at ScienceDirect

Atmospheric Environment

journal homepage: www.elsevier.com/locate/atmosenv

NO_x emissions from blasting operations in open-cut coal mining

Moetaz I. Attalla*, Stuart J. Day, Tony Lange, William Lilley, Scott Morgan

CSIRO Energy Technology, P.O. Box 330, Newcastle, NSW 2300, Australia

ARTICLE INFO

Article history:
Received 1 February 2008
Received in revised form 1 July 2008
Accepted 7 July 2008

Keywords:
NO_x
Open-cut mining
Australia
Miniaturised ultraviolet spectrometer
Mini-DOAS

ABSTRACT

The Australian coal mining industry, as with other industries is coming under greater constraints with respect to their environmental impacts. Emissions of acid gases such as NO_x and SO_x to the atmosphere have been regulated for many years because of their adverse health effects. Although NO_x from blasting in open-cut coal mining may represent only a very small proportion of mining operations' total NO_x emissions, the rapid release and high concentration associated with such activities may pose a health risk. This paper presents the results of a new approach to measure these gas emissions by scanning the resulting plume from an open-cut mine blast with a miniaturised ultraviolet spectrometer. The work presented here was undertaken in the Hunter Valley, New South Wales, Australia during 2006. Overall this technique was found to be simpler, safer and more successful than other approaches that in the past have proved to be ineffective in monitoring these short lived plumes. The average emission flux of NO_x from the blasts studied was about 0.9 kt t^{-1} of explosive. Numerical modelling indicated that NO_x concentrations resulting from the blast would be indistinguishable from background levels at distances greater than about 5 km from the source.

1. Introduction

Open-cut coal mining is widespread in the upper Hunter Valley in New South Wales (NSW) with several large mines operating within close proximity to the towns of Muswellbrook and Singleton. Consequently, there is community concern about the potential environmental impacts of mining on nearby populations.

Blasting, in particular, has the potential to affect areas outside the mine boundary and accordingly, vibration and dust emission limits are set in each mine's environmental licence. However, gaseous emissions of environmental concern, such as nitrogen dioxide (NO_2) may also be released during blasting operations. Currently, there are very little quantitative data relating to the magnitude of these emissions and it is not yet possible to determine if they contribute significantly to ambient levels in the main population centres.

The explosive ammonium nitrate/fuel oil (ANFO) is used almost universally throughout the open-cut coal mining industry. Under ideal conditions, the only gaseous products from the explosion are carbon dioxide (CO_2), water (H_2O) and nitrogen (N_2).

$$3NH_4NO_3 + CH_2 \rightarrow 3N_2 + CO_2 + 7H_2O \quad (1)$$

However, even quite small changes in the stoichiometry (either in the bulk material or caused by localised conditions such as moisture in the blast hole, mineral matter or other factors) can lead to the formation of substantial amounts of the toxic gases carbon monoxide (CO) and nitric oxide (NO) as shown.

$$2NH_4NO_3 + CH_2 \rightarrow 2N_2 + CO + 5H_2O \quad (2)$$

$$5NH_4NO_3 + CH_2 \rightarrow 4N_2 + 2NO + CO_2 + 7H_2O \quad (3)$$

In addition, some of the NO formed may oxidise in the presence of oxygen (O_2) to produce NO_2.

* Corresponding author.
E-mail address: moetaz.attalla@csiro.au (M.I. Attalla).

1352-2310/$ – see front matter Crown Copyright © 2008 Published by Elsevier Ltd. All rights reserved.
doi:10.1016/j.atmosenv.2008.07.008

$$2NO + O_2 \rightarrow 2NO_2 \quad (4)$$

Often in practice, large quantities of NO_2 are released from blasts which are observed as intense orange plumes.

Although these gases are not considered in their environmental licences, each mine is required to estimate annual emissions of CO, NO_x and SO_2 for the National Pollutant Inventory (NPI), compiled each year by the Australian government. These estimates are made by multiplying the amount of explosive consumed by an emission factor which is currently 8 kg t^{-1} for NO_x, 34 kg t^{-1} for CO and 1 kg t^{-1} for SO_2 (National Pollutant Inventory, 1999). These emission factors, however, are based on limited overseas data and are subject to high uncertainty.

Most of the studies which have examined NO_x formation from blasting have used blast chambers. The results from these studies do not necessarily correlate with what is observed during actual blasts. Few studies have attempted to measure NO_x emissions under actual field conditions, presumably because of the practical difficulties involved. Plumes from blasting lack confinement, can be very large in size and are affected by prevailing weather conditions. There is also a large quantity of dust associated with the blast and these factors combine to make physical sampling of the plume very difficult. There are also the obvious safety implications which restrict access to blast sites. Consequently, quantitative measurements of plume characteristics are generally unavailable. Nevertheless, it is important for mine operators, particularly when their operations are close to residential areas, to have some method for assessing NO_x formation and more importantly, predicting the severity of the NO_x plume. At present predictions of NO_x formation are subjective and are based on the blast engineer's knowledge of the area to be blasted (e.g. rock type, area of the mine, presence of water in the holes, etc.) and the ratings obtained from blasts performed under similar conditions. Quantitative flux estimations of NO_x released from a blast require measurement of concentration through the plume in both the horizontal and vertical axes.

Some of the options available to make these measurements are given in the following sections.

1.1. Physical sampling

Sampling of blasting fumes involves taking a sample of gas from the plume for subsequent analysis, which could be either on site or in an off site laboratory. Although physical sampling could in principle provide sufficient information to characterise a plume, there are a number of serious logistical problems with this approach:

- The size of the plume means that a large number of sample points would be required to sample across the width and height of the plume.
- The force of the explosion and the resulting debris would restrict the proximity of any sampling packages to the initial gas release.
- The potential toxicity of the plume; personnel cannot move through it to take samples, hence sampling stations must be fixed prior to the blast. This means that the path of the plume must be anticipated before the blast.

1.2. Continuous analysis

Another option is to use portable analysers to measure NO_x concentrations in real time. There are, however, disadvantages with this approach since a sample of the plume must be presented to the instrument for analysis. Usually a pump draws air through a small diameter tube into the instrument, but to achieve the necessary spatial characterisation of the plume, sample tubes would need to be positioned at various points throughout the plume. Thus many of the problems identified for the physical sampling would also apply to the use of continuous analysers.

1.3. Optical methods

There are several optical methods of analysis currently available that may be applicable to field measurements of NO_x. These include open-path Fourier Transform Infra-Red Spectroscopy (FT-IR), Correlation Spectroscopy (COSPEC) and Differential Optical Absorption Spectroscopy (DOAS). FT-IR has often been used in air pollution studies (e.g. Levine and Russwurm, 1994). It has also been used in mine situations to measure fugitive methane emissions. Kirchgessner et al. (1993) used open-path FT-IR (op-FT-IR) to estimate methane emissions from open-cut coal mines in the United States. The technique relies on passing a collimated infrared beam through ambient air over a path length of up to several hundred metres. In the Kirchgessner et al. (1993) study, the concentration of methane across the plume was measured then wind speed data and a Gaussian plume dispersion model were used to estimate the methane emission rate from the mine. These authors subsequently developed a modification of their method which improved its accuracy (Piccot et al., 1994, 1996). The improved method was essentially the same as described above except that methane concentrations were measured at several elevations to better characterise the plume.

In principle, open-path FT-IR could be used to measure NO_x in blast plumes since it is sensitive to NO, NO_2, and CO along with other gases. Infrared radiation is also strongly absorbed in many parts of the spectrum by both CO_2 and water which are very likely to be present in high concentrations in blast plumes and this may tend to obscure the NO_x signal. High resolution instruments may resolve at least some of the NO_x absorption lines, however, a more serious drawback with op-FT-IR is that the infrared beam would be substantially attenuated by the dust thrown up by the blast. In the period immediately after the blast when the dust level is very high it is likely that the IR beam would be completely blocked thus making measurements impossible.

Another well established optical method is Correlation Spectroscopy (COSPEC). The system was first described by Moffat and Milan (1971) and was designed to measure point source emissions of SO_2 and NO_2 from industrial plants but found a niche application in the measurement of SO_2 fluxes from volcanoes (Galle et al., 2002). The COSPEC system utilises a "mask correlation" spectrometer and was designed to measure vertical or slant columns using

sky-scattered sunlight. By traversing beneath plumes with the mobile instrument, the concentration of the column is calculated and, once multiplied by the plume velocity, produces a source emission rate. These instruments are limited to detecting only those species where masks are available. They also suffer from interferences from other atmospheric gases and light scattering from clouds or aerosols that can produce errors in column densities (Chalmers Radio and Space Science, website).

The DOAS technique is a relatively new technique that is gaining widespread acceptance as an air pollution monitoring method. Like the open-path FT-IR method, the DOAS can simultaneously measure concentrations of a number of species over path lengths which typically range from hundreds of metres to kilometres.

A DOAS, configured as an 'active system', Fig. 1, has three main parts – a light emitter, a light receiver and a spectrometer. The emitter sends a beam of light to the receiver (in some cases the emitter and receiver are contained in the same unit and the light beam is reflected off a remotely located passive reflector). The light beam contains a range of wavelengths, from ultraviolet to visible, although instruments are now available with an infrared source, which extends the range of compounds that can be detected. Different pollutant molecules absorb light at different wavelengths along the path between the emitter and receiver. The receiver is connected to the spectrometer which measures the intensity of the different wavelengths over the entire light path and through the data system converts this signal into concentrations for each of the species being monitored.

DOAS instruments are routinely used to measure SO_2, NO_2 and O_3.

More recently, advances in miniaturising UV–vis spectrometers has lead to the development of much more compact DOAS units, configured as a passive system (Fig. 1), which have come to be known as "mini-DOAS". The mini-DOAS system has so far been used mainly in the study of SO_2 fluxes in volcanic emissions (McGonigle et al., 2003).

2. Methodology

2.1. Field measurements

A portable DOAS (mini-DOAS) manufactured by Resonance Ltd was used in this study. The instrument covers a spectral range of 280–420 nm and can measure sub-part per million levels of NO_2 and SO_2. The unit, which comprises a telescope, scanning mirrors, calibration cells and a miniature CCD array spectrometer (Ocean Optics USB2000 spectrometer), is housed in a small package which is mounted on a tripod. Calibration of the instrument was carried out using the internal calibration cell. The concentration of the cell was equivalent 50 ppm m. No SO_x measurements were undertaken.

Data collection and processing were performed by Ocean Optics OOIBase32 software loaded in a laptop computer. This results in a more compact system that is easier to deploy at mine sites and provides greater flexibility in positioning the instrument in relation to the blast plume.

Prior to each monitored blast, a dark spectrum was collected by blocking light from entering the spectrometer and a scan was performed. To produce a reference spectrum, a further scan was performed in a clear sky background which contained background absorption from NO_2. The reference spectrum was required in order to determine the increase in concentration of NO_2 above ambient levels in the blast plumes.

The plume resulting from each blast was tracked with the spectrometer until the NO_2 concentration was indistinguishable from the surrounding sky. During each field measurement, the mini-DOAS and a video camera were positioned a safe operating distance from the blast at all times.

NO_2 concentrations in the plume were calculated by subtracting the dark spectrum from the measured spectrum and the reference spectrum using the supplied software.

The results obtained from the mini-DOAS are a path-averaged NO_2 concentration profile measured in units of parts per million metre (ppm m). The mini-DOAS results must be divided by the path length through the plume to yield a concentration. To estimate the amount of NO_2 released from each blast it was necessary to multiply the concentration by the volume of the plume. Hence it was necessary to estimate the dimensions of each plume.

All of the blasts monitored were video-taped using at least one, and sometimes two, video recorders. The distances between the cameras and the blast were measured by locating their positions with a handheld GPS receiver.

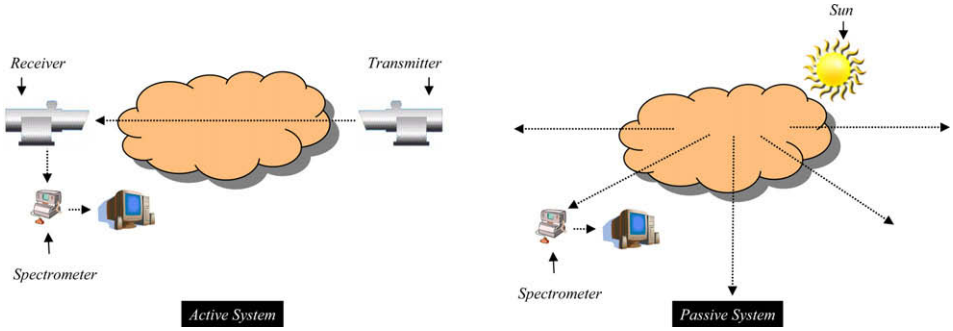

Fig. 1. Schematic diagram of DOAS systems operating in both active and passive modes.

Wind speed and directional data used to plot the directional path of the plume were obtained from a series of meteorological stations located around the mining lease. Simple trigonometry was employed to determine the distance from the video camera to the plume at the corresponding time intervals.

A rudimentary method of photogrammetry was then used to estimate the size of the plume based on still images extracted from the videos. Ratios of the plume to picture size in both the vertical and horizontal planes were made.

Once the plume to camera distance and the constraining angle for the plume is known, a crude three-dimensional estimate of the plume dimension was calculated using basic trigonometric functions. An example of the dimensions determined for a plume using this method is shown in Fig. 2.

Ground level measurements were carried out using a Greenline 8000 portable gas analyser. This instrument is capable of continuous, simultaneous analysis of O_2, CO_2, CO, SO_2, NO and NO_2. It is battery powered and can operate unattended for up to about 2 h. The instrument was calibrated against a standard gas mixture before each use. Data were logged on a laptop computer connected to the instrument.

For each experiment, the instrument was set up downwind of the blast in a location where the plume was expected to pass, but far enough away to avoid flying debris. The inlet probe was fixed at about 2 m above ground level.

It must be noted that selecting an appropriate location for the instrument was often difficult. In many cases, the wind conditions were quite variable, especially within the pit so it was not always possible to correctly anticipate the path of the blast plume. As well, the layout of the mine pit and safety considerations imposed constraints on where the instrument could be placed. Because of these problems, the plumes from many of the blasts did not pass over the analyser and data was not recorded.

2.2. Modelling

A simple modelling exercise was undertaken for this study to determine if the release of NO_2 from a blast could be of detriment to persons exposed to the plume within 5 km of the release. The results of this study are indicative and based on the assumption that the model used is appropriate. Modelling generally relies on local observational data to confirm the performance of the model. The difficulty in measuring emissions from mining blasts has meant that in this case the model is used as an indicator relying on the verifications used in the development of the chosen model. For this reason we have modelled concentrations directly downwind of theoretical blasts with AFTOX (Kunkel, 1991), a USEPA approved dispersion model (http://www.epa.gov/scram001/dispersion_alt.htm#aftox). The original DOS based QuickBasic code was transformed into Excel macros to enable many scenarios to be run.

AFTOX is a Gaussian Puff model developed for the United States Air Force to assess real time toxic chemical releases. The model uses information from US Air Weather Service (AWS) stations to calculate dispersion based on measured atmospheric conditions. As for all Gaussian models, the spread of pollutants is governed by dispersion coefficients in the horizontal (σ_y) and vertical (σ_z) directions. These coefficients depend on the atmospheric stability derived from the AWS data. In this study, the scenarios were modelled by predefining the wind speed and atmospheric stability classes. The wind speeds modelled ranged from very low (0.5 m s^{-1}) to moderate (10 m s^{-1}). Stability was modelled in six steps representing the standard Pasquill-Gifford stability classes, i.e. A–F, where A, B and C represent unstable conditions (where A is the most unstable), D is neutral and E and F are stable conditions. These stability classes are used to categorise the rate at which a plume will disperse. Unstable conditions might be found on a sunny day with light winds leading to rapid plume dispersion while the stable conditions may occur in clear skies with light winds and perhaps a temperature inversion present. Plume spread is slow in these circumstances.

AFTOX is operated by assuming an emission release from a single location. The emissions can be either continuous or instantaneous. In this study AFTOX was used to describe an area source by representing it as a large number of individual points. The area of the emission (i.e. the area over which the explosives were distributed) was

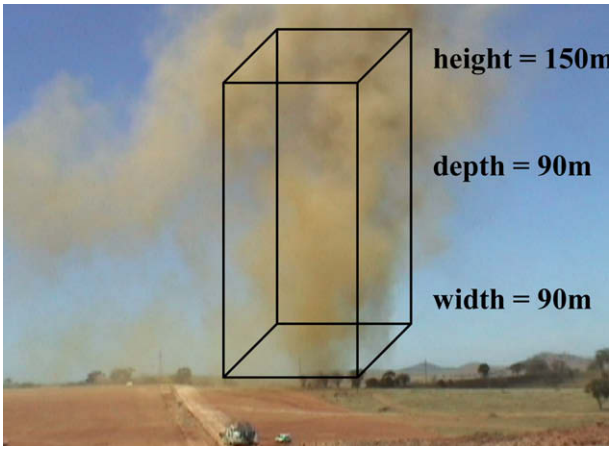

Fig. 2. Blast plume with estimated dimensions.

assumed to be 100 m × 200 m based upon sizes commonly observed during the field measurements. The area was subdivided into 10 m × 10 m units. Each square was represented by a point source with its source at the centre. In total, the area was modelled as 231 separate point sources (see Fig. 3). The total flux of emissions for the source was set at 100 kg. To estimate the maximum concentration and pollutant exposure values, the values should be multiplied by an appropriate scaling factor.

One hundred and twenty scenarios were modelled in which the 100 kg of emissions were spread randomly throughout the source area. A multi-stage process was employed for this task. In the first step, the total maximum number of points emitting was determined. This was defined by a random number between 20% and 80% of the maximum number of sources (in this case 231). The range chosen was an estimate from the portion of blasts that appeared to fume in conditions witnessed during this study. The total emission was then divided by this number. Each portion of the total emission was then placed randomly within the emission area. This process allowed certain points to receive multiple portions of the total emissions enabling the formation of hot spots. An example of one emission grid (Scenario 1 of 120) is displayed in Fig. 4.

Concentrations were determined for each of the 120 emission scenarios at distances of 200 m, 300 m, 400 m, 500 m, 750 m, 1 km, 1.25 km, 1.5 km, 2 km, 2.5 km, 3 km, 4 km and 5 km from the origin of the source. A concentration was determined for a number of discrete times that encompassed the complete plume travelling past the receptor. Further the concentrations were determined at 21 locations 10 m apart in a plane parallel and directly downwind of the source area (see Fig. 3). An average concentration from each of the receptors was determined; in this case with N equal to 21.

$$C^{*} = \frac{1}{N}\sum_{i=1}^{N} C_i \tag{5}$$

The average for each scenario was then used to create an ensemble average and standard deviation for the entire run (i.e. $N = 120$).

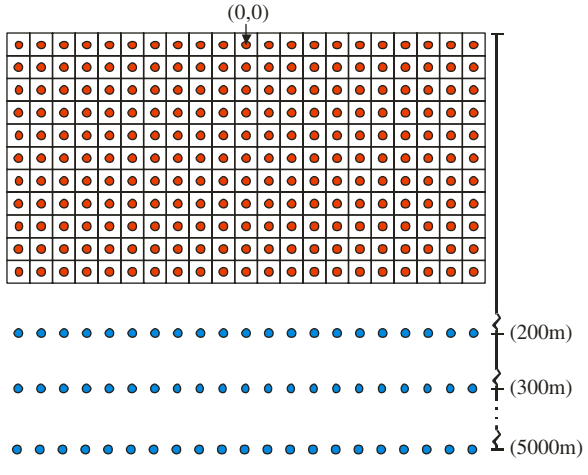

Fig. 3. Emission grid and receptor array setup.

$$\overline{C} = \frac{1}{N}\sum_{j=1}^{N} C_j^{*} \tag{6}$$

$$\sigma_{\overline{C}} = \frac{1}{N}\sum_{j=1}^{N}\left(C_j^{*} - \overline{C}\right)^2 \tag{7}$$

$$C_{\max} = \max_{k=1}^{N}[\overline{C}_k] \tag{8}$$

A dosage expressed in ppm s was determined from the times when the ensemble average plume travelled past the receptors located at each distance downwind of the source. Again N represents each discrete time step (dt) where $C' \neq 0$.

$$C_{\text{dose}} = \sum_{k=1}^{N}(\overline{C}_k)\mathrm{d}t \tag{9}$$

The relative variation for the dosage is provided by similarly treating the ensemble standard deviation.

$$\sigma_{\text{dose}} = \sum_{k=1}^{N}(\sigma_{\overline{C}k})\mathrm{d}t \tag{10}$$

3. Results and discussion

3.1. Field measurements

Plume measurements were made using the mini-DOAS spectrometer at two open-cut mine sites located in the Hunter Valley. The combination of the spectral analysis and the plume estimation technique allowed for NO_2 concentration and mass flux estimates to be made remotely, totally eliminating the requirement of physical sampling.

An example of the spectral output produced by the mini-DOAS is shown in Fig. 5. The spectral output consists of the NO_2 concentration (ppm m) as a function of time. The figure also contains a series of photographs depicting the formation of a blast plume at time intervals of 70, 110, 163, 250 and 350 s post-blast initiation. It is worth noting the change in intensity of the colour of plume and size as a function of time.

Reliable concentration measurements with the mini-DOAS may only be made when the spectrometer is aimed into a sky background above the horizon from the point of observation. In this example, a peak concentration of 580 ppm m was achieved in 163 s post-blast initiation (third image from the left). At this time the plume has risen above the horizon from the point of observation. The plume to mini-DOAS distance at this stage is approximately 500 m, with an estimated plume depth of 105 m. This results in a NO_2 concentration of 5.6 ppm at that particular stage of the plumes' dispersion.

After 350 s, the plume is barely visible and is now estimated to be approximately 650 m from the mini-DOAS unit. The plume depth has increased to 125 m with

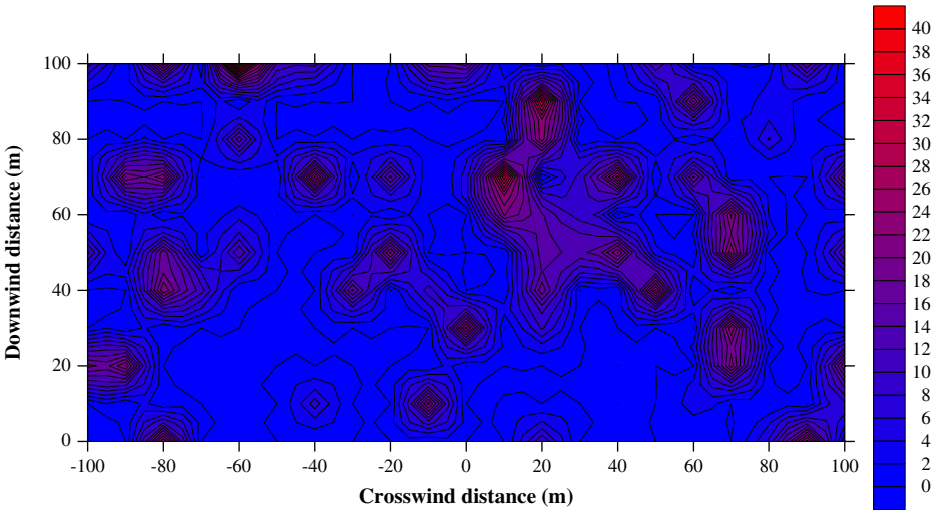

Fig. 4. Example of emission grid for 1 of the 120 scenarios modelled (the scale on the right hand side refers to NO_2 concentration in ppm).

a corresponding increase in plume volume by a factor of two. This expansion of the plume corresponds to a decrease in NO_2 concentration to 2.8 ppm.

At 360 s the plume was no longer visible to the eye and was lost for a short period of time to the mini-DOAS. This, however, was rectified with scanning of the sky with the spectrometer until the invisible plume was tracked for a further period.

Results for all plumes monitored during field work at both mine sites are given in Table 1. The table gives the peak NO_2 concentration as measured by the mini-DOAS above the horizon. Also given in the table is the plume volume at peak concentration and the calculated mass of NO_2 released from the blast. The mass of ANFO typically used in a blast was on average 210 tonnes, ranging from 60 to 565 tonnes. The explosive was distributed over an area of typically 200 m × 100 m containing approximately 200 bole holes with 200 mm diameter and to a depth of 25 m.

From the table the maximum NO_2 concentrations were found to range from 0 to about 7 ppm. This range of concentrations translated to 0–63.3 kg of NO_2 in the plume. However, no correlation can be made between blast charge and NO_2 levels.

During the measurements with the mini-DOAS ground level measurements were also carried out using a portable combustion gas analyser (Greenline 8000) to augment the airborne measurements made by the mini-DOAS. For NO_2 the ground level measures were higher than those observed using the mini-DOAS at higher altitudes. When the results of both measurement methods were applied to

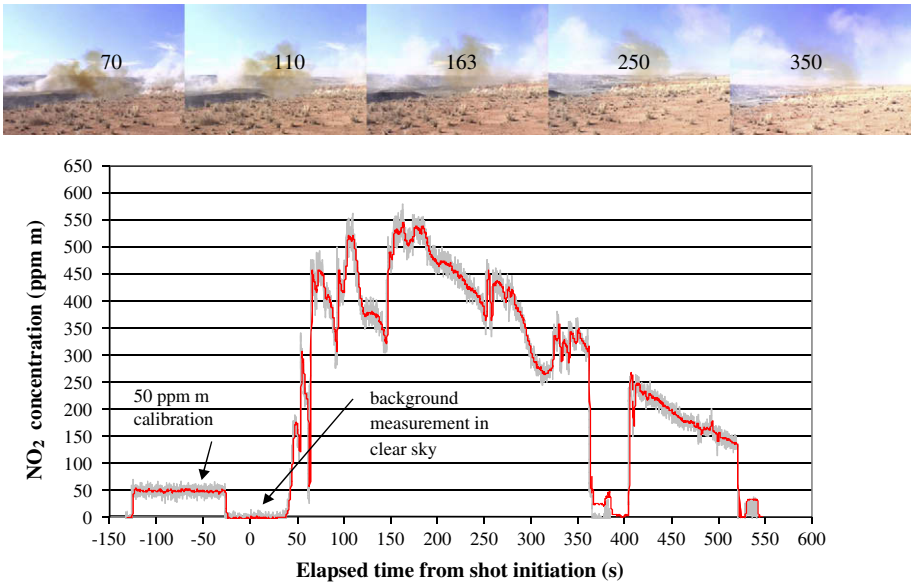

Fig. 5. Typical NO_2 spectrum demonstrating plume colour characteristics relative to concentration level.

Table 1
Through plume measurement results

Date	Total ANFO charge (t)	Peak NO_2 Conc (ppm)	Plume volume ($m^3 \times 10^{-6}$)	Mass of NO_2 (kg)	Emission flux (kg t^{-1} ANFO)		
					NO	NO_2	NO_x
12/12/2005	281	3.7	1.4	9.9	0.5	0.03	0.6
13/12/2005	150	0.4	5.3	3.7	0.4	0.03	0.4
14/12/2005	119	0.0	0.0	0.0	0.0	0.00	0.0
21/12/2005	229	1.0	4.4	7.9	0.6	0.04	0.6
22/12/2005	211	0.0	0.0	0.0	0.0	0.00	0.0
23/12/2005	222	0.0	0.0	0.0	0.0	0.00	0.0
5/01/2006	177	1.0	0.2	0.4	0.0	0.00	0.0
6/01/2006	275	1.1	15.3	30.6	1.8	0.12	1.9
12/01/2006	225	1.6	6.2	18.3	1.3	0.08	1.4
18/01/2006	169	1.3	1.7	0.2	0.4	0.02	0.4
23/01/2006	139	2.1	4.2	16.7	1.9	0.12	2.0
25/01/2006	155	0.4	4.4	2.9	0.3	0.02	0.4
30/01/2006	132	0.7	5.3	7.1	0.8	0.05	0.9
22/02/2006	224	0.0	0.00	0.0	0.0	0.00	0.0
1/03/2006	194	1.6	20.6	63.3	5.0	0.32	5.3
12/05/2006	362	6.5	1.9	23.3	1.0	0.06	1.1
15/05/2006	131	0.3	3.2	1.7	0.2	0.01	0.2
19/05/2006	168	0.0	0.00	0.0	0.0	0.00	0.0
30/05/2006	100	0.8	0.00	1.0	0.0	0.00	0.0
1/06/2006	365	0.7	3.5	4.9	0.2	0.01	0.2
6/06/2006	145	0.8	11.5	17.5	1.9	0.12	2.0
15/06/2006	60	0.0	0.00	0.0	0.0	0.00	0.0
26/06/2006	254	4.3	0.3	2.1	0.1	0.01	0.2
27/06/2006	212	5.6	0.9	10.0	0.7	0.04	0.7
28/06/2006	241	0.0	0.00	0.0	0.0	0.00	0.0
6/07/2006	565	2.8	2.7	14.0	0.4	0.03	0.4
13/07/2006	184	7.0	1.0	12.6	1.1	0.07	1.2

dispersion modelling techniques strong agreement was observed.

Point measurements which were made on Greenline 8000 indicated that a loose relationship existed between NO and NO_2 concentration. Although a strong correlation was not found, there is a general trend of increasing NO_2 with increasing NO. It was generally found that the relative proportion of NO to NO_2 from our data set was 27 to 1. This

Table 2
Maximum calculated NO_2 concentrations downwind of source

	200 m	300 m	400 m	500 m	750 m	1000 m	1250 m	1500 m	2000 m	2500 m	3000 m	4000 m	5000 m
WSPD = 0.5 m s^{-1}													
Stab A	83.0	30.0	14.4	7.9	2.5	0.9	0.4	0.2	0.1	0.0	0.0	0.0	0.0
Stab B	145.8	69.3	40.8	25.4	10.1	4.8	2.6	1.6	0.7	0.4	0.2	0.1	0.1
Stab C	219.4	122.0	80.8	55.9	26.8	14.3	8.6	5.6	2.8	1.6	1.0	0.5	0.3
Stab D	321.1	201.5	146.0	113.1	64.6	40.2	26.1	18.6	10.5	6.7	4.5	2.4	1.4
Stab E	390.2	267.4	204.3	165.5	109.6	75.9	54.6	41.3	26.4	17.9	12.7	7.1	4.5
Stab F	464.1	339.8	269.0	222.6	154.5	114.9	88.6	69.7	50.4	37.0	27.8	16.7	11.0
WSPD = 3 m s^{-1}													
Stab A	78.5	29.1	14.2	7.7	2.4	0.9	0.4	0.2	0.1	0.0	0.0	0.0	0.0
Stab B	137.6	67.7	39.7	25.1	10.0	4.8	2.6	1.6	0.7	0.4	0.2	0.1	0.1
Stab C	211.6	118.7	77.6	55.2	26.0	14.0	8.6	5.6	2.8	1.6	1.0	0.5	0.3
Stab D	312.5	197.9	143.2	110.0	62.5	39.3	26.1	18.2	10.5	6.7	4.5	2.4	1.4
Stab E	383.0	267.0	202.1	162.6	106.3	73.7	54.1	40.3	26.1	17.7	12.5	7.2	4.5
Stab F	461.5	344.6	268.4	220.8	151.1	112.3	86.1	67.6	48.9	36.4	27.5	16.6	11.0
WSPD = 7.5 m s^{-1}													
Stab A	62.5	25.5	13.0	7.3	2.3	0.9	0.4	0.2	0.1	0.0	0.0	0.0	0.0
Stab B	111.9	56.1	34.2	22.6	9.4	4.6	2.6	1.6	0.7	0.4	0.2	0.1	0.1
Stab C	173.3	100.4	66.5	47.7	23.8	13.2	8.2	5.4	2.7	1.6	1.0	0.5	0.3
Stab D	261.2	167.9	122.1	92.3	54.8	35.3	23.7	17.2	10.1	6.5	4.4	2.3	1.4
Stab E	325.9	232.2	175.8	139.6	89.5	63.8	46.7	36.0	23.9	16.8	12.1	7.0	4.4
Stab F	394.6	302.7	237.0	194.3	132.2	96.1	73.3	59.0	43.6	33.3	25.7	15.8	10.5
WSPD = 10 m s^{-1}													
Stab A	53.0	22.6	11.9	6.9	2.3	0.9	0.4	0.2	0.1	0.0	0.0	0.0	0.0
Stab B	92.3	49.7	31.0	20.9	9.0	4.5	2.5	1.5	0.7	0.4	0.2	0.1	0.1
Stab C	140.1	84.2	57.7	42.1	21.7	12.6	7.9	5.3	2.7	1.6	1.0	0.5	0.3
Stab D	205.5	138.3	102.4	79.9	48.6	31.8	22.1	16.4	9.7	6.4	4.3	2.3	1.4
Stab E	254.0	184.0	143.0	116.4	78.0	56.2	42.6	33.1	22.7	16.0	11.6	6.9	4.4
Stab F	306.8	235.8	189.6	157.9	109.9	82.8	64.5	52.2	40.0	30.9	24.0	15.2	10.2

relationship enabled the estimation of the NO fluxes in the blast plume with a reasonable level of confidence.

The results obtained in this study are the only published quantitative data available on blast plume gas composition that the authors are aware of and it is useful to compare them to the emission factors currently used for NPI estimates.

Based on the NO_2 measurements and estimates of NO, the flux for NO_x was calculated to be in the range of 0.04–5.3 kg t^{-1} ANFO. The average flux level for all the blast plumes measured was 0.9 kg t^{-1}. This figure is considerably lower than the current NPI emission factor which is 8 kg t^{-1}.

3.2. Modelling

Results of the modelling runs are summarised in Table 2 and show the peak NO_2 concentrations (ppm) at various points downwind of the blast for the six atmospheric stability classes considered.

Examples of the modelled data are plotted in Fig. 6 and Fig. 7. In Fig. 6 a plot is displayed for the concentration estimate of one scenario at a distance of 200 m from the source origin and for a wind speed of 2 m s^{-1} and a stability class C. In this plot 21 lines are shown representing the dose received directly downwind of the source at the locations displayed in Fig. 3. In this figure it is apparent that there is a considerable difference in the concentration predicted at each of the 21 receptors. It should be noted that the distance of 200 m is defined from the origin of the source area (0, 0) as displayed in Fig. 3. At this distance emission sources at 100 m will cause significantly higher concentrations than those occurring at positions toward the origin. In comparison the concentrations predicted at the receptor array 1 km from the source show more normally defined distributions with maxima occurring towards the middle receptors as a result of crosswind diffusion. Receptors toward the edge of the sample array receive less crosswind influence and are, therefore, smaller in concentration. Also apparent in these two figures is the considerable difference in the predicted peak concentrations with the values at 1 km up to 25 times lower than at 200 m. When viewing Table 2, the peak values at 5 km approach ambient levels for all but the most stable conditions which are quite commonly over predicted with Gaussian models. For future studies it is recommended that a long path technique on a mining lease boundary may provide both a measure of the model accuracy as well as a direct measure of the impact in areas directly surrounding the mining area.

The data presented in this study represent a dose directly downwind of the source and as such are a worst case scenario for exposure. The averages of the 21 receptors (i.e. the average concentration directly downwind of the source) for each of the 120 scenarios modelled were used to determine the selected data. The number of scenarios modelled was arbitrarily chosen to allow 10 scenarios to be run on each machine in a cluster of 12 computers. The maximum concentration in Table 2 is the maximum ensemble average obtained from the average of the 21 receptors for the 120 scenarios modelled. Maximum concentrations at individual locations directly downwind of hot spots are obviously higher than the values reported in this table.

When viewing Table 2 it is apparent that the peak concentrations drop dramatically as the receptor moves away from the source. It is also apparent that the peak concentrations vary little as a function of wind speed although the plume width will vary. In AFTOX a downwind concentration is determined in two steps. In the first step the size of the initial plume envelope is estimated. In its default mode AFTOX determines the size of the envelope (assumed to be a cylinder of equal height and width) from the magnitude of the emission rate. In this report the size is set at 10 m to match the grid structure used for the area

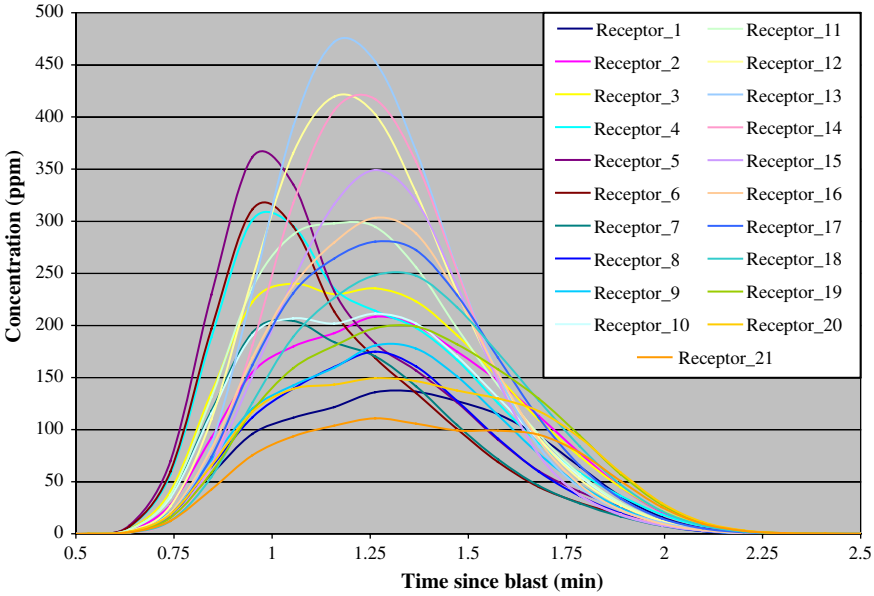

Fig. 6. Calculated NO_2 concentration profiles 200 m from source.

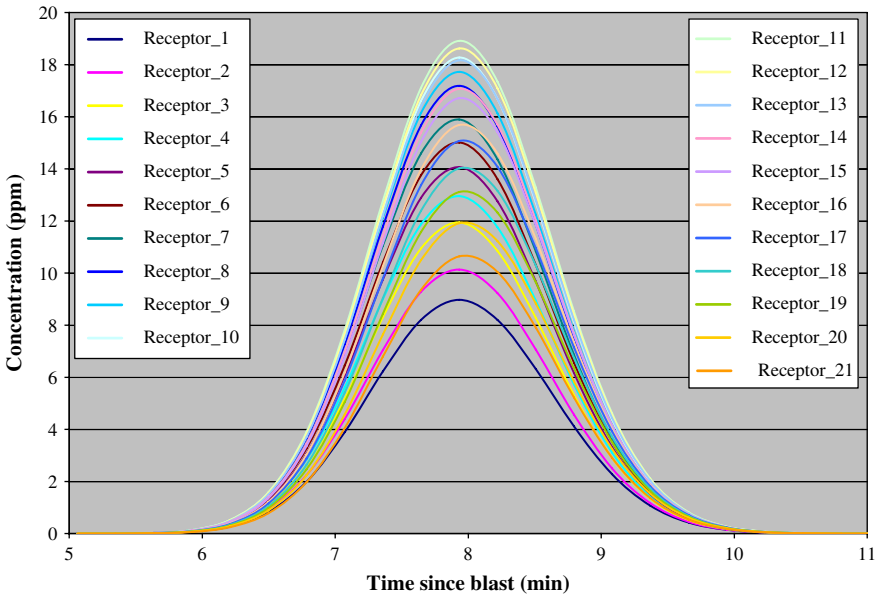

Fig. 7. Calculated NO_2 concentration profiles 1 km from source.

source. AFTOX in this regard ignores the effect of wind speed on the size of the initial envelope and as such the initial concentration of the plume is identical irrespective of wind speed by ignoring longitudinal (i.e. downwind) spread of the initial release. In the second step the concentration downwind of the initial release is determined by estimating the growth of a puff in three dimensions which in this case explicitly includes longitudinal plume spread which is assumed to be equal to the degree of crosswind spread. The degree of this spread is determined solely from the prescribed atmospheric stability class which ignores any wind speed dependence.

While the peak concentrations are similar, the dose received at a receptor is linearly dependent on wind speed. Emissions released into an atmosphere with higher wind speeds result in a receptor receiving doses for a smaller period of time. It should be noted that some of the differences in the peak concentrations displayed in Table 2 result from the number of discrete time steps used to calculate the concentrations. This was set at 25 intervals between the onset and finish of a plume as it passes by the receptor. This time is dependent on atmospheric stability and the distance from the source. In AFTOX, the puffs are assumed to disperse in the direction of plume travel proportionally with the degree of crosswind spread. As such, portions of the plume arrive before and after the main bulk of the emissions and the effect clearly demonstrated in Figs. 6 and 7. The moderate number of discrete times modelled to capture this effect while generally adequate may have led to a degree of variation particularly at larger distances from the source.

Again it should be noted that the modelled figures assume an area wide flux of 100 kg which is larger than observed in the blast recorded during this study. It should also be noted that while some of the concentrations are high close to the source the concentration at a particular location occurs for a brief period of time which is determined by the wind speed.

4. Conclusions

A portable open-path spectroscopic method was found to be effective for measuring NO_2 emissions from blasting. Overall this technique was found to be simpler, safer and more successful than other approaches that in the past have proved to be ineffective in monitoring these short lived plumes.

Quantitative measurements of NO_2 in plumes from blasting were made at two open-cut mines. The results showed that NO_2 was present in most of the plumes but in relatively low concentrations (typically ranging between 0 and 7 ppm). The highest concentration measured during all the field campaigns was about 17 ppm at ground level.

Based on field measurements, the emission factor currently used in compiling the Australian National Pollutant Inventory was found to be approximately eight times greater than that observed in our investigation. This would suggest that an over estimation of NO_x is made if the current factor is used.

Numerical modelling of the behaviour of plumes resulting from blasting was made to assess the possible downwind concentrations of NO_2. These results were compared to ambient NO_x measurements made in Muswellbrook.

- Modelling results were consistent with concentration measurements within the plumes at relatively short distances from the blast (i.e. up to about 1 km).
- Ambient monitoring did not detect NO_x events that could be attributed to individual blasts. Modelling suggested that these emissions would be very low at

distances greater than 5 km from the blast and may be indistinguishable from background levels; typically of the order of several parts per billion, in most cases.

Acknowledgements

We gratefully acknowledge the financial support of the Australian Coal Association Research Program (ACARP) and the staff at the Hunter Valley mine sites.

References

Chalmers Radio, Space Science. The optical remote sensing group. Available from: <http://www.rss.chalmers.se/ors/ >.

Galle, B., Oppenheimer, C., Geyer, A., McGonigle, A.J.S., Edmonds, M., Horrocks, L., 2002. A miniaturised ultraviolet spectrometer for remote sensing of SO_2 fluxes: a new tool for volcano surveillance. Journal of Volcanology and Geothermal Research 119, 241–254.

Kirchgessner, D.A., Piccot, S.D., Chadha, A., 1993. Estimation of methane emissions from a surface coal mine using open-path FTIR spectroscopy and modelling techniques. Chemosphere 26, 23–44.

Kunkel, B.A., 1991. AFTOX 4.0 – The Air Force Toxic Chemical Dispersion Model – A User's Guide. PL-TR-91-2119, Environmental Research Papers No. 1083, Phillips Laboratory, Directorate of Geophysics, Air Force Systems Command, Hanscom AFB, MA 01731-5000, p. 62.

Levine, S.P., Russwurm, G.M., 1994. Fourier transform infrared optical remote sensing for monitoring airborne gas and vapour contaminants in the field. Trends in Analytical Chemistry 13, 263–266.

Moffat, A.J., Milan, M.M., 1971. The applications of optical correlation techniques to the remote sensing of SO_2 plumes using sky light. Atmospheric Environment 5, 677–690.

McGonigle, A.J.S., Thomson, C.L., Tsanev, V.I., Oppenheimer, C., 2003. A simple technique for measuring power station SO_2 and NO_2 emissions. Atmospheric Environment 38, 21–25.

National Pollutant Inventory, 1999. Emission Estimation Technique Manual for Explosives Detonation and Firing Ranges. Environment Australia. Available from: <http://www.npi.gov.au/handbooks/approved_handbooks/fexplos.html>.

Piccot, S., Masemore, S., Ringler, E., Srinivasan, S., Kirchgessner, D., Herget, W., 1994. Validation of a method for estimating pollution emission rates from area sources using open-path FTIR spectroscopy and dispersion modelling techniques. Journal of the Air & Waste Management Association 44, 271–279.

Piccot, S., Masemore, S., Ringler, E., Bevan, W.L., Harris, D.H., 1996. Field assessment of a new method for estimating emission rates from volume sources using open-path FTIR spectroscopy. Journal of the Air & Waste Management Association 46, 159–171.